Nanoscale Res Lett (2010) 5:68–73
DOI 10.1007/s11671-009-9444-1

NANO EXPRESS

High Methanol Oxidation Activity of Well-Dispersed Pt Nanoparticles on Carbon Nanotubes Using Nitrogen Doping

Wei-Chuan Fang

Received: 9 June 2009 / Accepted: 24 September 2009 / Published online: 9 October 2009

Abstract Pt nanoparticles (NPs) with the average size of 3.14 nm well dispersed on N-doped carbon nanotubes (CNTs) without any pretreatment have been demonstrated. Structural properties show the characteristic N bonding within CNTs, which provide the good support for uniform distribution of Pt NPs. In electrochemical characteristics, N-doped CNTs covered with Pt NPs show superior current density due to the fact that the so-called N incorporation could give rise to the formation of preferential sites within CNTs accompanied by the low interfacial energy for immobilizing Pt NPs. Therefore, the substantially enhanced methanol oxidation activity performed by N-incorporation technique is highly promising in energy-generation applications.

Keywords Methanol oxidation activity · N-doped carbon nanotubes · Energy-generation applications

Introduction

Hybrid nanocomposites containing carbon nanotubes (CNTs) have attracted much attention when each constituent component provides different functions for specific applications [1]. Although the properties of some CNT-containing nanocomposites have been investigated [2], the interface and transport issues in systems still remain a challenge, particularly in electrochemical (EC) systems [3]. As shown from previous studies, CNTs have great potential as electrode materials in direct methanol fuel cells (DMFCs) [4]; however, the surface of CNTs is chemically inert and therefore the uniform dispersion of metal nanoparticles (NPs) is impossible. It is necessary to modify the CNTs prior to the support for capturing electrocatalysts such as Pt- or Pt-based NPs [5, 6]. In general, the chemical modification is accomplished by acid oxidation using some oxygen-containing functional groups [7, 8]. These routes are obviously complicated and result in the formation of pollutants. Meanwhile, the mechanical properties of modified CNTs are affected as well.

Recently, chemical doping of CNTs is an attractive proposition for a wide range of potential applications. Extrinsic doping of the tube surfaces can give rise to the formation of localized electronic states [9] and makes the tubes chemical active; hence, N-doped CNTs are less stable than their pure carbon counterparts, breaking easily [10] and oxidizing at lower temperature than undoped CNTs [11] due to the fact of nitrogen atoms as localized defects, which will be energetically less stable than a pure carbon lattice. Moreover, it will make CNT surfaces chemically active by chemical modification [12]. Their active surfaces mean they can be dispersed in a range of solvents not possible with undoped tubes [13]. On the other hand, it is found that N-doped CNTs only show the metallic behavior with a strong donor peak just above the Fermi level [14], unlike undoped CNTs which exhibit a variety of metallic and semiconducting behavior depending on their chirality.

Doping provides a way to activate regions along the tube wall and surface reactivity is increased. This opens up the possibility of doping techniques not available in traditional three-dimensional materials, notably chemical functionalization of tubes, tube coating with metal ions [15, 16]. Accordingly, it suggests that the concept of N incorporation would be critical in chemical modifications of CNTs.

W.-C. Fang (✉)
Materials and Chemical Research Laboratories, Industrial Technology Research Institute, Chutung 310, Taiwan
e-mail: d893513@alumni.nthu.edu.tw

These properties possessed by N-doped CNTs could render a new type of desirable catalyst support and electrode material in DMFCs.

In this work, we have developed a simple chemical method to directly immobilize Pt NPs on N-doped CNTs without any pre-surface modification. The electrocatalytic properties of Pt-loaded N-doped CNTs for methanol oxidation are examined and an obvious catalytic activity is obtained, indicating their potential ability in energy-generation applications.

Experimental

Synthesis of Nanocomposites

For CNT array preparation, Fe film was deposited on Si substrates by sol–gel method as catalyst prior to CNTs growth step. Then, aligned CNTs were grown on the pre-coated substrates by microwave plasma-enhanced chemical-vapor deposition (MPECVD). The MPECVD growth was performed with microwave power at 2 kW; CH_4, N_2, and H_2 as source gases; and the substrate temperature of 1000 °C. To study N-doping effect, N_2 gas was not fed into the chamber during CNTs growth. For Pt deposition, DC sputtering under Ar gas flow was performed.

Characterization

For material analyses, a JEOL 6700 field-emission scanning electron microscope (FESEM), a JEOL JEM-2100F field-emission transmission electron microscope (FETEM), X-ray diffractometry (XRD) (PHILIPS PW1700), and X-ray photoelectron spectroscopy (XPS) (VG Scientific ESCALAB 250) were utilized. EC measurements were carried out using an Autolab potentiostat system in a three-electrode set up using Pt wire and reversible hydrogen electrode (RHE) as the counter and reference electrode, respectively. The electrolyte used was 1 M CH_3OH and 0.5 M H_2SO_4 at room temperature.

Results and discussion

The XRD pattern of Pt NPs on N-doped and undoped CNTs is shown in Fig. 1. It can be found that the peak (111) of Pt NPs on N-doped and undoped CNTs is revealed. According to the Debye–Scherrer equation, the grain size is inversely proportional to the full width at half maximum (FWHM) of diffraction peak in XRD pattern. Therefore, the FWHM of N-doped CNTs is broadened, which suggests that the grain size of Pt NPs on N-doped CNTs is smaller than that on undoped ones.

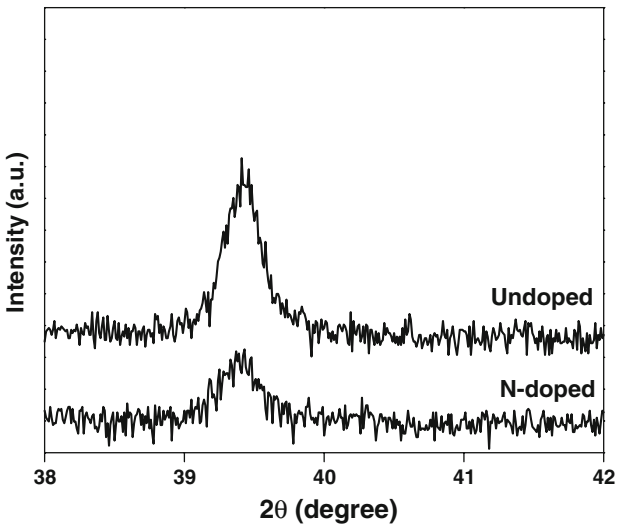

Fig. 1 X-Ray diffraction pattern of Pt nanoparticles (NPs) immobilized on N-doped carbon nanotubes (CNTs) and undoped ones

To understand the bonding of Pt NPs on N-doped and undoped CNTs, the surface scan of XPS spectrum is examined as shown in Fig. 2. In the XPS survey spectrum, four different bonding configurations of C 1s, Pt 4d, and Pt 4p in Pt NPs dispersed on N-doped and undoped CNTs have been found. It shows that N bonding is present in Pt NPs dispersed on N-doped CNTs, which suggests that N atom does incorporate with CNTs and the relevant discussion would be performed in advance.

As seen in Fig. 3a, C 1s XPS spectrum of Pt NPs on N-doped and undoped CNTs is measured. The binding energy of Pt NPs on N-doped and undoped CNTs is 284.6 and 284.4 eV, respectively. From the report of Matter et al., the binding energy of C 1s XPS spectrum for sp^2

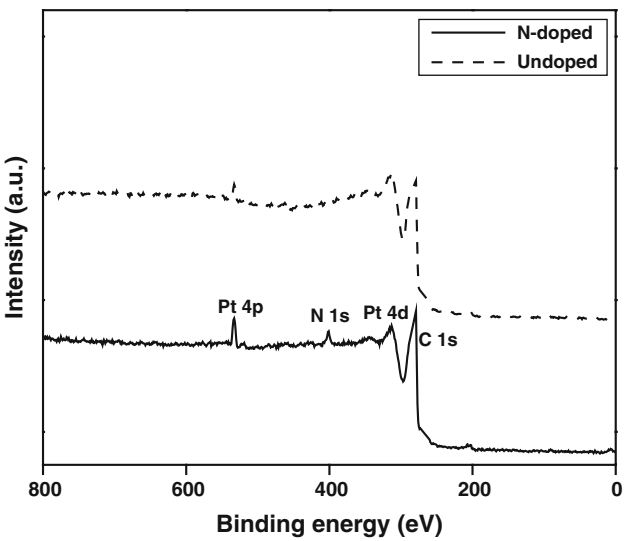

Fig. 2 Surface scan of Pt NPs immobilized on N-doped CNTs and undoped ones

hybridization in pyridine (C_5H_5N) is located at 285.5 eV and it also appears in the nanostructured N-doped carbon [17–22] Based on the above results, it is probably supposed that the C–N bonding could be embedded within N-doped CNTs.

However, Pt 4f XPS spectrum of Pt NPs on N-doped and undoped CNTs looks the same, as depicted in Fig. 3b. This means that no electron transfer of Pt NPs on N-doped CNTs occurs; accordingly, if the EC behavior of Pt NPs on N-doped CNTs proceeds, the other possibility besides the electronic modification can be explained. To see the formation of N bonding, N 1s XPS spectrum of Pt NPs on N-doped and undoped CNTs is displayed in Fig. 3c. From C 1s and N 1s XPS spectrum, the N/C ratio of N-doped CNTs is about 2:98. It is found that the formation of N bonding is evident in Pt NPs deposited on N-doped CNTs. In general, the N 1s XPS spectrum can be deconvoluted with four N-based bonding configurations inclusive of pyridinic N (398.6 eV), pyrrolic N (400.5 eV), quaternary N (401.3 eV), and pyridinic N^+–O^- (402–405 eV) in N-doped CNTs. Among those N-induced bonding configurations, pyridinic and pyrrolic N are quite important in the enhancement of electrical properties of NTs and dispersion of Pt NPs on N-doped CNTs.

Figure 4 shows the cross-sectional FESEM images of Pt NPs on N-doped and undoped CNTs. It can be seen that both CNTs look similar in terms of density or height. As shown in Fig. 4a, Pt NPs are uniformly distributed on the sidewalls of N-doped CNTs. By contrast, those Pt NPs agglomerate on the surface of undoped CNTs in Fig. 4b. From the SEM images of Pt NPs on N-doped and undoped CNTs, it can be seen that well-dispersed Pt NPs on CNTs can be realized using N doping.

To further see the deposition of Pt NPs on N-doped and undoped CNTs, one-single N-doped and undoped CNT are shown in Fig. 5. As displayed in Fig. 5a, the uniform dispersion of Pt NPs are immobilized on N-doped CNTs due to the defects induced by N doping. On the contrary, if CNTs do not contain N bonding, the interfacial energy of NTs would be much higher. As a result, the degree of dispersion for Pt NPs on CNTs is substantially reduced; therefore, the Pt NPs will agglomerate as shown in Fig. 5b. It provides the important information that Pt NPs are uniformly dispersed on the sidewalls of CNTs incorporated with N. Moreover, the particle-size distribution of Pt NPs dispersed on N-doped CNTs is performed in Fig. 5c. Clearly, the particle diameter of Pt NPs ranges from 2 to 4.5 nm and the estimated average size is about 3.14 nm calculated from the depicted diagram, which infers that the ultrafine Pt NPs immobilized on CNTs without any chemical modification can be achieved using N incorporation.

For EC activity characterization of Pt NPs on N-doped and undoped CNTs, Fig 6 exhibits the EC properties of Pt NPs on CNTs under different conditions. It is examined at

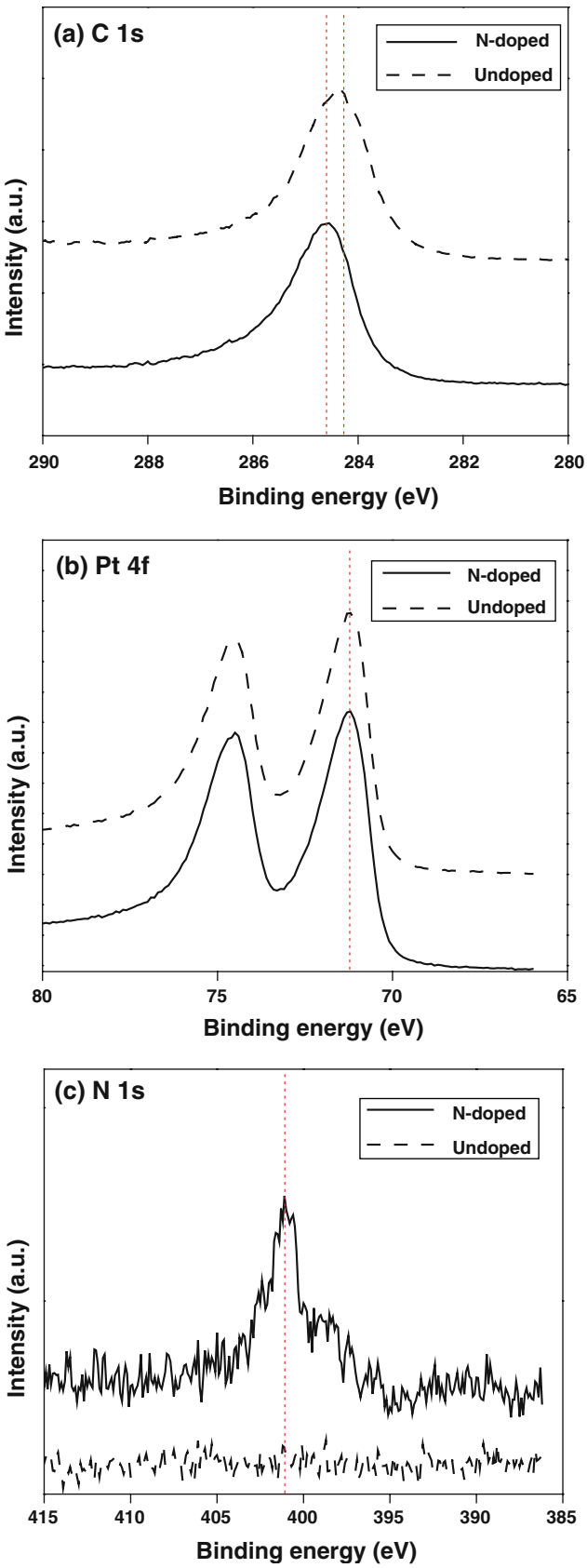

Fig. 3 XPS spectrum of Pt NPs immobilized on N-doped CNTs and undoped ones

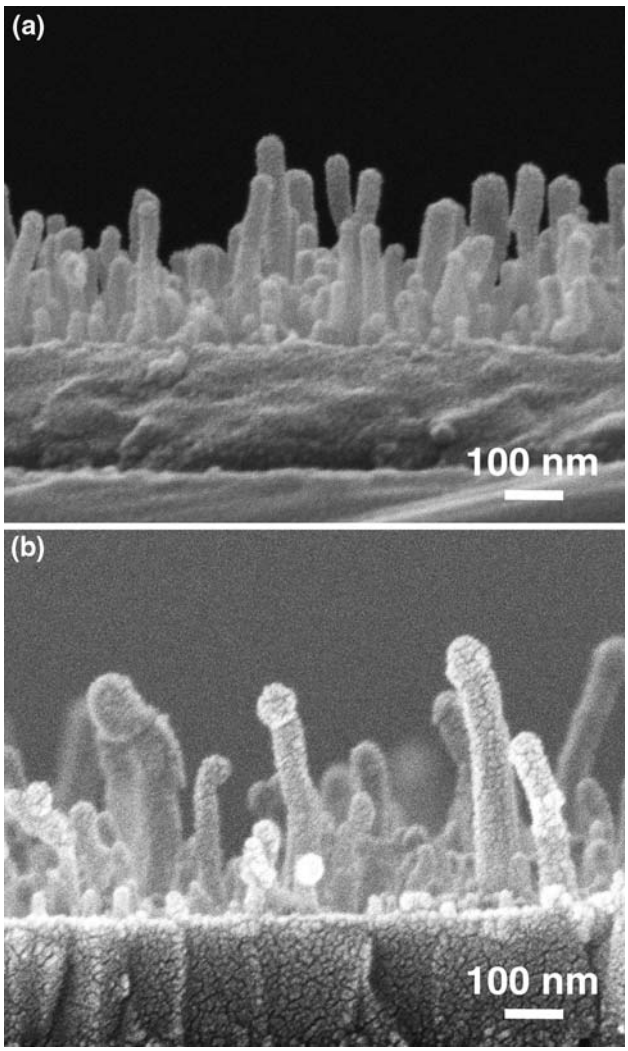

Fig. 4 Cross-sectional scanning electron microscope images of Pt NPs immobilized on **a** N-doped CNTs and **b** undoped ones

the scan rate of 50 mV/s in 1 M CH_3OH and 0.5 M H_2SO_4. In Fig. 6a, the CV diagram of Pt NPs dispersed on N-doped CNTs shows the better performance compared with that of those NPs on undoped ones. In addition, Fig. 6b also reveals that the onset potential of Pt NPs on N-doped CNTs is lower than that of those NPs on undoped ones. The relevant EC properties of those two specimens are summarized in Table 1. The weight of Pt particles on undoped and N-doped CNTs is estimated about 83 and 122 μg/cm^2, respectively. From the resultant data, it is evident that the EC characteristics of Pt NPs on N-doped CNTs are superior to that on undoped ones; hence, the so-called N doping could efficiently promote the uniform dispersion of Pt NPs on CNTs accompanied by the enhanced methanol-oxidation activity.

From the above studies, N-incorporation effect has very important impact on the enhancement of EC properties for

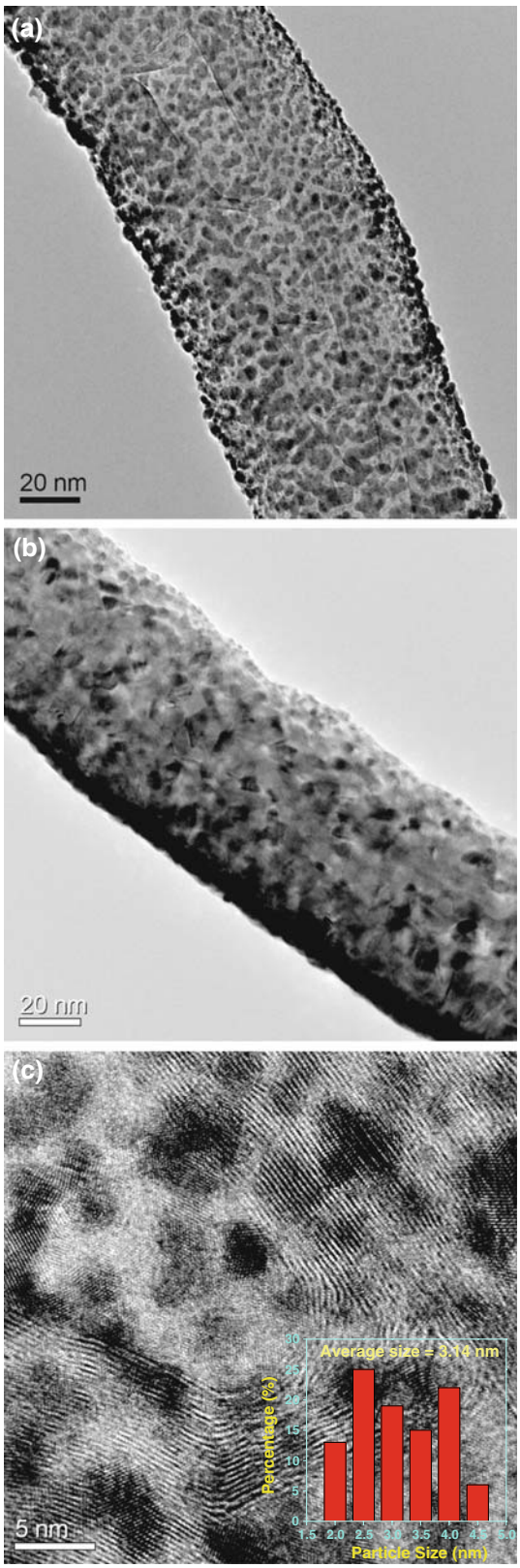

Fig. 5 Transmission electron microscope (TEM) images of Pt NPs immobilized on **a** N-doped CNTs and **b** undoped. **c** The magnified TEM image of (**a**)

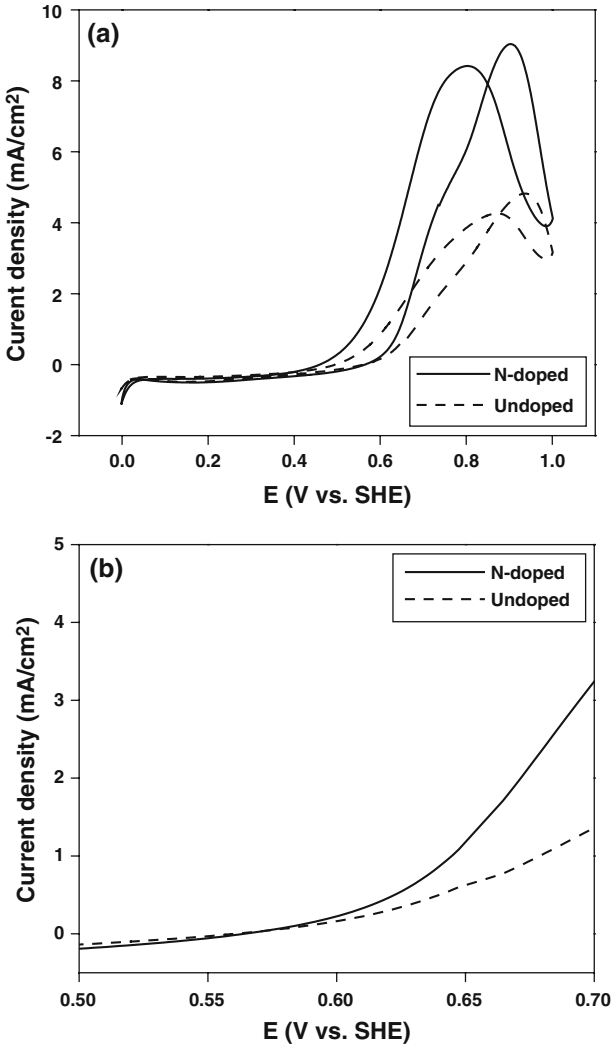

Fig. 6 **a** Electrochemical activity of PtNPs immobilized on N-doped CNTs and undoped ones and bonset potential for methanol oxidation

Table 1 EC performance of Pt particles immobilized on N-doped and undoped CNTs

Specimens	Forward onset potential (V)	Forward peak current density (A/g)
Pt/N-doped CNTs	0.58	75
Pt/undoped CNTs	0.63	55

DMFC applications. The N-doping technique efficaciously immobilizes extrinsic electrocatalysts such as Pt NPs and put them regularly on the sidewalls of CNTs as demonstrated from SEM and TEM images. To elaborate the mechanism, the depicted diagrams are displayed in Fig. 7. In Fig. 7a, the scheme shows that the N doping generates the two defects inclusive of pyrrolic and pyridinic N.

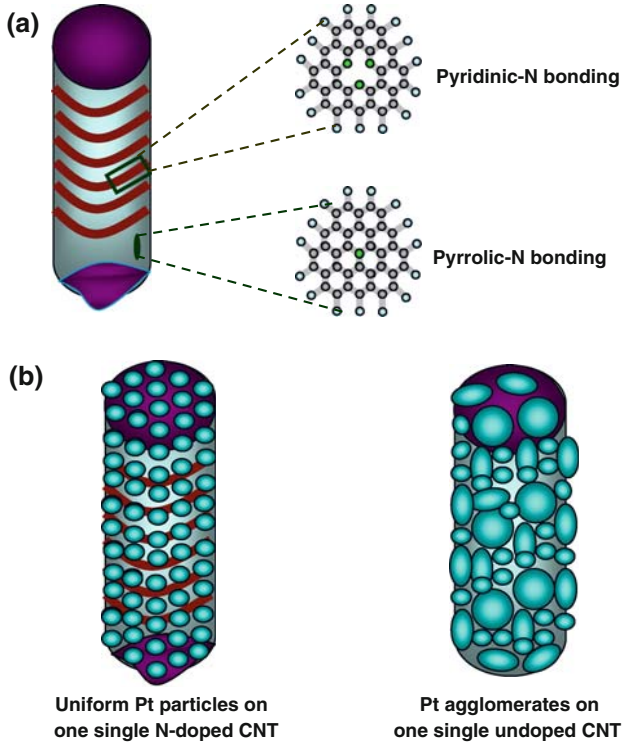

Fig. 7 Schematic diagram of **a** N-doping mechanism and **b** Pt NPs immobilized on N-doped CNTs and undoped ones

Pyrrolic N is on the surface of CNTs and pyridinic N is on the node of bamboo-like tubes. In fact, pyrrolic N is highly correlated with dispersion degree of Pt NPs and EC activity performances. As shown in Fig. 7b, if N atoms are not doped, the surface of CNTs becoming quite stable and electrochemically inert give rise to the agglomerate formation of Pt NPs on CNTs accompanied by inferior EC activity. However, the aggregate problem can be removed as N doping is fulfilled due to the hydrophilic interface generated by preferential defect sites in CNT surfaces. Accordingly, it generates the high EC activity followed by the enhanced methanol oxidation property [23–27]. On the other hand, N-doped CNTs show only the metallic behavior with a strong donor peak just above the Fermi level [14], unlike undoped tubes which exhibit a variety of metallic and semiconducting behavior depending on their chirality. This is also helpful in the enhancement of energy-generation efficiency for DMFC applications.

Conclusion

The enhanced EC activity of Pt NPs immobilized on N-doped CNTs directly grown on Si substrate has been established. Structural properties show the characteristic bonding peaks of N within CNTs providing good support for uniform distribution of Pt NPs. In EC activity, N-doped

CNTs covered with Pt NPs show superior current density at the scan rate of 50 mV/s. This is due to the fact that the so-called N incorporation could be used to create preferential sites of CNTs with low interfacial energy for grabbing Pt NPs. Thus the substantially enhanced methanol oxidation activity produced by N-incorporation technique is very promising in energy-generation applications.

Acknowledgments The author is grateful for the support of the Industrial Technology Research Institute (No. 7101QV3320).

References

1. G.L. Che, B. Brinda, R. Lakshmi, E. Fisher, C.R. Martin, Nature **393**, 346 (1998)
2. H. Tang, J.H. Chen, Z.P. Huang, D.Z. Wang, Z.F. Ren, L.H. Nie et al., Carbon **42**, 191 (2004)
3. W. Ehrfeld, Electrochim. Acta **348**, 2857 (2003)
4. W.Z. Li, C.H. Liang, W.J. Zhou, J.S. Qiu, Z.H. Zhou, G.Q. Sun et al., J. Phys. Chem. B **107**, 6292 (2003)
5. W.C. Choi, S.I. Woo, M.K. Jeon, J.M. Sohn, M.R. Kim, H.J. Jeon, Adv. Mater. **17**, 446 (2005)
6. Z.L. Liu, J.Y. Lee, W.X. Chen, M. Han, L.M. Gan, Langmuir **20**, 181 (2004)
7. M. Kaempgen, M. Lebert, M. Haluska, N. Nicoloso, S. Roth, Adv. Mater. **20**, 616 (2008)
8. A. Kuznetsova, I. Popova, J.T. Yates, M.J. Bronikowski, C.B. Huffman, J. Liu et al., J. Am. Chem. Soc. **123**, 10699 (2001)
9. C.P. Ewels, M. Glerup, J. Nanosci. Nanotechnol. **5**, 1345 (2005)
10. M. Glerup, J. Steinmetz, D. Samaille, O. Stéphan, S. Enouz, A. Loiseau et al., Chem. Phys. Lett. **387**, 193 (2004)
11. C.J. Lee, S.C.L. yu, H.W. Kim, J.H. Lee, K.I. Cho, Chem. Phys. Lett. **359**, 115 (2002)
12. K.Y. Jiang, L.S. Schadler, R.W. Siegel, X. Zhang, H. Zhang, M. Terrones, J. Mater. Chem. **14**, 37 (2004)
13. M. Holzinger, J. Steinmetz, S. Roth, M. Glerup, R. Graupner, AIP Conference Proceedings (IWEPNM) **786**, 129 (2005)
14. R. Czerw, Nano Lett. **1**, 457 (2001)
15. R.S. Lee, H.J. Kim, J.E. Fischer, J. Lefeb vre, M. Radosa vljevic, J. Hone et al., Phys. Rev. B **61**, 4526 (2000)
16. M. Bockrath, J. Hone, A. Zettl, P.L. McEuen, A.G. Rinzler, R.E. Smalley, Phys. Rev. B **61**, 10606 (2000)
17. X.A. Zhao, C.W. Ong, Y.C. Tsang, C.W. Wong, P.W. Chan, C.L. Choy, Appl. Phys. Lett. **66**, 2652 (1995)
18. U. Gelius, R.F. Heden, J. Hedman, B.J. Lindberg, R. Manne, R. Nordberg, Phys. Scr. **2**, 70 (1970)
19. C.D. Wagner, W.M. Riggs, L.E. Davis, J.F. Moulder, G.E. Muilenberg, in *Handbook of X-ray Photoelectron Spectroscopy*, vol 40 (1978), p. 45
20. P.H. Matter, E. Wang, M. Arias, E.J. Biddinger, U.S. Ozkan, J. Mol. Catal. A Chem. **264**, 73 (2007)
21. P.H. Matter, L. Zhang, U.S. Ozkan, J. Catal. **239**, 83 (2006)
22. P.H. Matter, U.S. Ozkan, Catal. Lett. **109**, 115 (2006)
23. W.C. Fang, W.L. Fang, Chem. Commun. **41**, 5236 (2008)
24. W.C. Fang, J. Phys. Chem. C **112**, 11552 (2008)
25. W.C. Fang, Nanotechnogy **19**, 165705 (2008)
26. W.C. Fang, K.H. Chen, L.C. Chen, Nanotechnogy **18**, 485716 (2007)
27. W.C. Fang, O. Chyan, C.L. Sun, C.T. Wu, C.P. Chen, K.H. Chen et al., Electrochem. Commun. **9**, 239 (2007)